AIP | Biomicrofluidics
Fundamentals, Perspectives & Applications
#1 ORIGINAL RESEARCH JOURNAL IN THE FLUID AND PLASMA PHYSICS CATEGORY

The microfluidics of the eccrine sweat gland, including biomarker partitioning, transport, and biosensing implications

Z. Sonner, E. Wilder, J. Heikenfeld, G. Kasting, F. Beyette, D. Swaile, F. Sherman, J. Joyce, J. Hagen, N. Kelley-Loughnane, and R. Naik

Citation: Biomicrofluidics **9**, 031301 (2015); doi: 10.1063/1.4921039
View online: http://dx.doi.org/10.1063/1.4921039
View Table of Contents: http://scitation.aip.org/content/aip/journal/bmf/9/3?ver=pdfcov
Published by the AIP Publishing

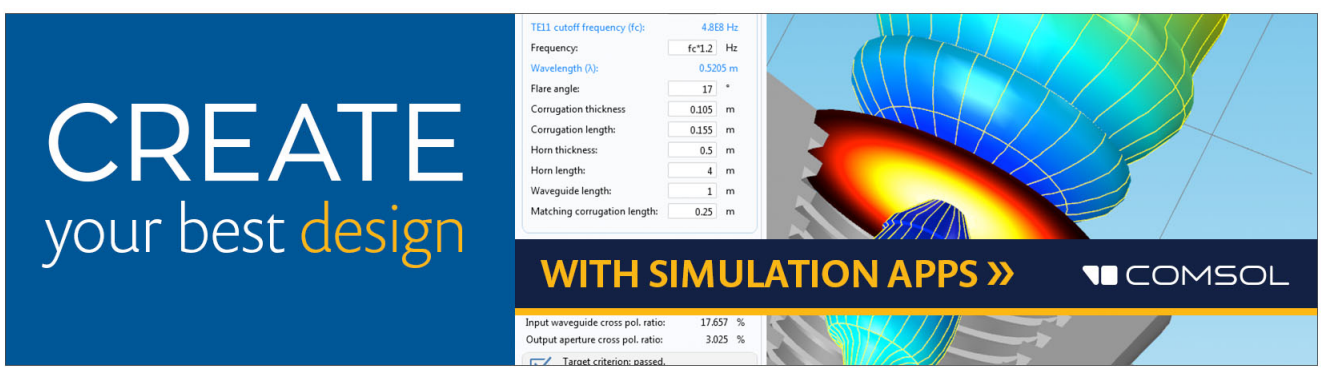

The microfluidics of the eccrine sweat gland, including biomarker partitioning, transport, and biosensing implications

Z. Sonner,[1,a)] E. Wilder,[2,a)] J. Heikenfeld,[1,b)] G. Kasting,[2] F. Beyette,[1] D. Swaile,[3] F. Sherman,[4] J. Joyce,[4] J. Hagen,[5] N. Kelley-Loughnane,[5] and R. Naik[6]

[1]*Department of Electrical Engineering and Computer Systems, University of Cincinnati, Cincinnati, Ohio 45221, USA*
[2]*Winkle College of Pharmacy, University of Cincinnati, Cincinnati, Ohio 45267, USA*
[3]*P&G Sharon Woods Innovation Center, Cincinnati, Ohio 45241, USA*
[4]*P&G Beckett Ridge Technical Center, West Chester, Ohio 45069, USA*
[5]*711 Human Performance Wing, Human Effectiveness Directorate, Air Force Research Laboratory, Wright-Patterson Air Force Base, Dayton, Ohio 45233, USA*
[6]*Functional Materials Division, Materials and Manufacturing Directorate, Air Force Research Laboratory, Wright-Patterson Air Force Base, Dayton, Ohio 45233, USA*

(Received 2 April 2015; accepted 30 April 2015; published online 15 May 2015)

Non-invasive and accurate access of biomarkers remains a holy grail of the biomedical community. Human eccrine sweat is a surprisingly biomarker-rich fluid which is gaining increasing attention. This is especially true in applications of continuous bio-monitoring where other biofluids prove more challenging, if not impossible. However, much confusion on the topic exists as the microfluidics of the eccrine sweat gland has never been comprehensively presented and models of biomarker partitioning into sweat are either underdeveloped and/or highly scattered across literature. Reported here are microfluidic models for eccrine sweat generation and flow which are coupled with review of blood-to-sweat biomarker partition pathways, therefore providing insights such as how biomarker concentration changes with sweat flow rate. Additionally, it is shown that both flow rate and biomarker diffusion determine the effective sampling rate of biomarkers at the skin surface (chronological resolution). The discussion covers a broad class of biomarkers including ions (Na^+, Cl^-, K^+, NH_4^+), small molecules (ethanol, cortisol, urea, and lactate), and even peptides or small proteins (neuropeptides and cytokines). The models are not meant to be exhaustive for all biomarkers, yet collectively serve as a foundational guide for further development of sweat-based diagnostics and for those beginning exploration of new biomarker opportunities in sweat.
[http://dx.doi.org/10.1063/1.4921039]

I. INTRODUCTION

The concept of using sweat for non-invasive access to biomarkers and solutes in blood is far from new, with large volumes of clinical work showing promising results as far back as the 1940s and 1950s. However, outside of cystic fibrosis (CF) diagnostics for increased sweat chloride levels[1,2] and testing for the metabolites of illicit drugs,[3,4] sweat remains relegated mainly to the lab and clinic. Both the significant opportunities and frustrations with sweat as a diagnostic tool are succinctly summarized by Bravo and Castro:[5] "*The main limitations of sweat as*

[a)]Z. Sonner and E. Wilder contributed equally to this work.
[b)]Author to whom correspondence should be addressed. Electronic mail: heikenjc@ucmail.uc.edu

clinical sample are the difficulty to produce enough sweat for analysis, sample evaporation, lack of appropriate sampling devices, need for a trained staff… normalization of the sampled volume."

In part, many of these issues are now being resolved by bringing low-cost wearable sensors into nearly immediate contact with sweat as it emerges onto skin.[6–14] This not only improves convenience and eliminates evaporative issues causing misleading increases in biomarker concentrations but also it is powerful as many biomarkers in collected biofluids degrade in as little as 10–20 min.[15] Wearables can also easily measure the change in sweat generation rate by skin impedance.[16–20] However, sweat generation rate does not predict actual biomarker sampling intervals without a detailed microfluidic and transport model between the sweat glands and sensors.

The lack of biomarker partitioning and microfluidic transport models for sweat also impairs discovery of new biomarker opportunities in sweat. Most historical studies use classical and comparatively crude clinical techniques such as collection of large sweat volumes in bags or textiles. As a result, many biomarker opportunities are possibly discarded prematurely due to an apparent lack of correlation between blood and sweat. For example, as is frequently the case, if the transport rate of a biomarker into sweat is passive (diffusive) and slower than the rate at which the biomarker is advectively transported to the skin surface, then an unknown dilution of the biomarkers can confound the experimental results. On the other hand, other studies at initial glance can provide data which is false-positive. For example, consider lactate, which is of great interest in both athletics[11,21,22] and critical care applications. The metabolic activity of a hard-working sweat gland itself creates abundant lactate which dominates over lactate diffusion from plasma.[2,23] High exertion exercise tests can therefore show a spike in lactate correlating with exercise intensity (sweat rate), but this does not necessarily represent the anaerobic state of the body.[24–26]

In addition to concerns with sweat rate dependence or metabolic relationships, there are also issues of contamination from the surface of the skin. For instance, it has been shown that glucose levels in sweat do trend with glucose levels in blood.[27] However, a severe limitation is that glucose diffusing from the uppermost layers of skin into the wet (sweaty) skin surface can completely confound sweat glucose correlation with blood. This further highlights the need for microfluidic models to inspire technological designs[28] that can isolate sweat from skin surface contaminants.

It is clear that sweat biosensing can benefit greatly from foundational models of the eccrine sweat gland. In particular, engineering-driven models are especially needed given the current watershed commercialization moment in bringing low-cost sensors into contact with skin. Presented are the microfluidics of the eccrine sweat gland which is critical for biomarkers with strong sweat flow rate dependence. Additionally, the model shows that flow rate and biomarker diffusion determine the effective sampling rate of biomarkers at the skin surface (chronological resolution). Also provided in this work are several example models for biomarker partitioning from blood into sweat, including ions (Na^+, Cl^-, K^+, NH_4^+), small molecules (ethanol, cortisol, urea, and lactate), and even peptides or small proteins (neuropeptides and cytokines). These models are based on decades of prior research in the dermatological and related bioscience fields. Reviewing these models will clearly show that biomarker partitioning can be highly unique to each biomarker (passive, active, or self-generating) and that correlation with blood depends on understanding the overall partitioning and microfluidic transport mechanisms. Our hypothesis is that the microfluidic and partitioning models presented within can serve as a foundational guide for more advanced models, for further development of sweat-based diagnostics and for those beginning exploration of new biomarker opportunities in sweat. In addition, the models will benefit those pursuing even broader types of on-skin products such as cosmetics, anti-perspirants, garments, wearable electronics, and medical adhesives. Finally, this paper may prove useful to those exploring other biomarker sources, such as saliva[4,29–32] or tears,[33] for which there are many parallels to eccrine sweat.

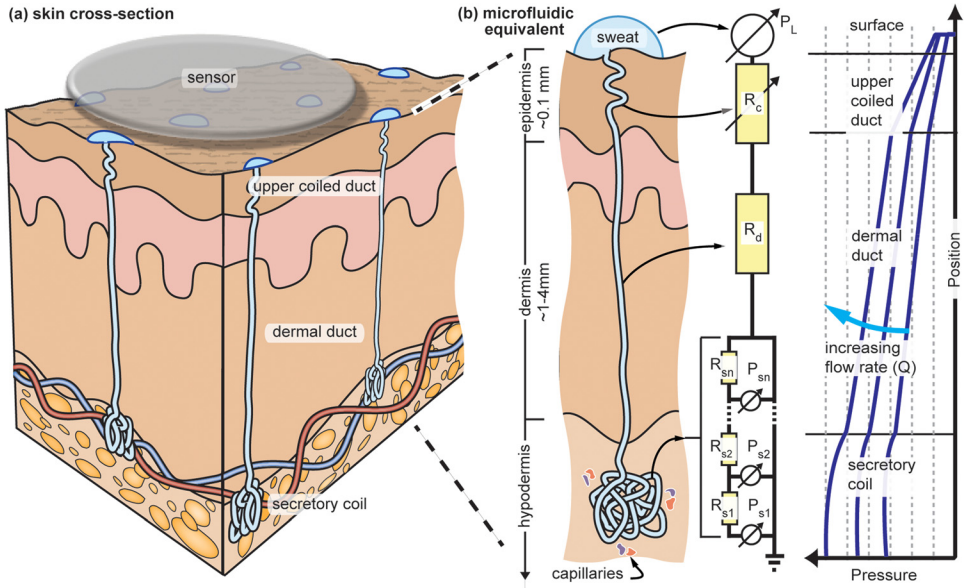

FIG. 1. Structure of the human sweat gland showing the (a) skin cross-section and (b) microfluidic equivalent.[34]

II. ULTRASTRUCTURE OF THE ECCRINE SWEAT GLAND

The ultrastructure of the eccrine gland must first be understood, as it has significant bearing on microfluidic transport and biomarker partitioning. The human eccrine sweat gland comprises several geometrically distinct portions, the secretory coil, the dermal duct, and the upper coiled duct, as shown in Figure 1. The upper coiled duct is also often referred to as the acrosyringium. In this region, the sweat duct expands in diameter slightly, until it emerges at the surface of the skin.[1,35,36]

Typical ranges for the physical dimensions of the human eccrine sweat gland are shown in Table I. These dimensions also have the potential to vary due to differences in gender, age, and race.[35–37] The largest portion of the eccrine sweat gland is the secretory coil, which can be upwards of 700 μm in diameter in its natural bundled state and with an extended length of several millimeters. The inner-diameters of the secretory coil and ductal regions are referred to as the lumen, ranging from 5 μm to 10s of μm.

Top-down cross-sectional illustrations of the secretory coil and dermal duct are shown in Figure 2. These cross-sections are important, as they are the interface through which biomarkers partition into new sweat. As shown in Figure 2(a), the secretory coil contains three primary cells: the clear (secretory), dark (mucoid), and myoepithelial (supportive) cells.[1,2,38] In comparison, the dermal duct contains only a bilayer of basal and luminal cells[1,38] as shown in Figure 2(b). Clear cells are hypothesized to be the dominant source of sweat secretion due to the abundance of mitochondria present within the cell[2] (see Subsection IV A on Na^+ and Cl^- partitioning). Dark cells, however, are believed to be involved in membrane-cellular transport and may also have the ability to act as clear cells, themselves.[2] Myoepithelial cells are thought to act as a supportive network between the basolateral membrane.[2] Regarding the dermal duct, the luminal cells form a semi-cuticular border with many microvilli protruding into the lumen of the duct, which increases the effective surface area of the cells for absorption or secretion.[2] The basal cells in the dermal duct are characterized with abundant mitochondria, also suggesting a highly active role in sodium reabsorption (see Subsection IV A on Na^+ and Cl^- partitioning).[1] Other physical descriptors of sweat glands and their densities across the body are listed in Table I. A more exhaustive review can be found elsewhere.[1,45] Notice how the axilla (armpit) is excluded. Even though the axilla has an eccrine gland density[36] of ~100 to 200 glands/cm^2,

TABLE I. Dimensions and additional physical descriptors for eccrine sweat glands.

Descriptor	Value (μm)	References
Secretory Coil		
Length	2000–5000	38
Outer diameter	60–120	36, 38
Inner diameter	5–40	36, 42
Total bundled (coiled) diameter	500–700	36
Dermal (straight) duct		
Length	~2000	36
Outer diameter	50–80	36
Inner diameter	10–20	36
Upper coiled duct (Acrosyringium)		
Length	200–300	36
Outer diameter	120	36
Inner diameter	20–60	36

Descriptor (units)	Value	References
Sweat surface tension (mN/m)	71.8	39
Composition of sweat (% water)	99	36
Maximum hydrostatic pressure (kN/m^2)	70	35, 39–41
Typical sweat rate range (ηL/min/gland)	<1–20	35
Number of glands/individual ($\times 10^6$)	1.6–5	2, 36, 43, 44

Approximate eccrine sweat gland densities[45]

Location	Approximate gland density (cm^{-2})
Toe	550
Palm, finger	250
Forehead, forearm	150
Abdomen, back, legs	100

it is rich with apocrine glands[46] which have a different secretion process that could confound eccrine sweat measurements and is therefore beyond the scope of this work.[45]

III. MICROFLUIDIC MODEL FOR THE ECCRINE GLAND

This section builds upon a much more simplified pressure-driven model we previously published for an *in-vitro* skin and sweat mimic.[47] Water will be used for all microfluidic parameters, as sweat is 99% water[36] (Table I). Regarding the hydraulic capability of the sweat gland itself, the gland is able to produce its greatest hydrostatic pressures in excess of an impressive 72 kN/m^2 *in-vivo* when chemically stimulated by pilocarpine iontophoresis[41] or methacholine,[35] measured by coupling a single gland with a stop flow pressure meter.[41] This pressure corresponds with sweat rates approaching 20 ηl/min/gland. Natural high sweat rates are more typically in the range of 5–10 ηl/min/gland.[26]

For each change in diameter along the length of the sweat gland, there will be also be a change in the pressure differential which occurs over this region. This is plotted qualitatively in Figure 1(b) as the plot of pressure vs. position along the length of the sweat gland. Assuming a constant circular cross-section for each sub-region of the gland, fluid flow can be modeled according to Poiseuille flow theory. This assumption is seemingly valid considering the structural support of the myoepithelium which resists pressure fluctuations.[2] One can then calculate the fluid resistance in each region according to[47,48]

$$R = \frac{128\mu L}{\pi d^4}, \tag{1}$$

where R is the fluid resistance for a specific geometry, μ is the viscosity, L is the length of the region, and d is the diameter of the circular cross-section. In this instance, the fluid resistance R can be used to calculate the pressure differential inside the gland by[47]

$$P = R \cdot Q, \tag{2}$$

where P is the pressure differential in the region of interest and Q is the volumetric flow rate. Beyond the secretory coil, Q is assumed to be constant along the *ductal* length of the sweat gland at an instance of time, and hence a linear pressure drop with distance. However, in Figure 1(b), the pressure drop in the *secretory coil* is shown as non-linear because Q increases with distance as more sweat is added to the secretory coil with distance (i.e., the pressure-drop due to fluid

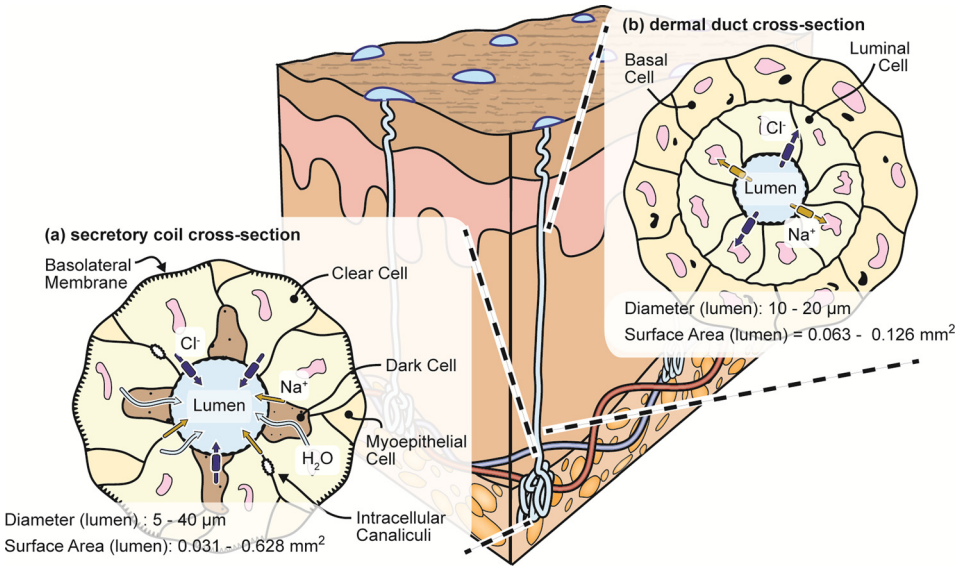

FIG. 2. Cross-sectional and top-down illustration of the (a) secretory coil and (b) dermal duct.[1,2,38]

resistance increases with distance to the end of the secretory coil). Therefore, microfluidically, the secretory coil itself can be modelled as a network of fluid (pressure) sources P_{sn} and fluid flow resistors R_{sn} (Figure 1(b)). The dermal duct (R_d) and partially upper coiled duct (R_c) can then be modeled as simple fluid flow resistors as they lack fluid source regions (Figure 1(b)). The diameter of the upper coiled duct (acrosyringium) near the skin surface can change as a result of swelling (hydration) of the stratum corneum;[49,50] hence, R_c is variable as shown in Figure 1(b). However, a significant increase in resistance in R_c is limited to regions of the body with a very thick stratum corneum (e.g., think of those skin surfaces which wrinkle after a long swim in the pool like the finger tips). Interestingly, this swelling is the same mechanism that is at least partially exploited in many types of antiperspirants utilizing glycols which swell the skin to the point where the flow of sweat is effectively restricted or even pinched off by R_c.

Finally, the external most pressure in Figure 1(b) is representative of the Laplace pressure P_L. P_L arises due to a combination of the surface tension of sweat and the generally convex curvature of the sweat meniscus as it emerges onto skin[47,51]

$$P_L = \frac{2\gamma \cos\theta}{a}, \tag{3}$$

where P_L is the Laplace pressure, γ is the surface tension of sweat, θ is the contact angle of the sweat on the skin surface, and a is the radius of the base of the droplet. For most applications, sweat covers the skin such that P_L reduces to zero (a is infinite) or is physically wicked away by textiles such that P_L is effectively negative in value. Equation (3) can also be used to show that the maximum pressure generated by the eccrine gland of $\sim$70 kN/m^2 is adequate to push sweat even through a super-hydrophobic pore ($\theta = 180^\circ$) that is only 4 μm in diameter ($a = 2\,\mu$m). Therefore, sweat glands are clearly capable of acting as the pressure pump if sweat needs to be driven by pressure into a microfluidic device for sampling.

The generation of sweat from a single gland is not steady in flow rate, rather it is pulsating. This is illustrated in Figure 3 which provides time-lapse photos of several active human eccrine glands on the forefinger of co-author Swaile. The droplets undergo water evaporation, dry skin water re-absorption, and possibly spreading on skin that cannot be directly observed in the photos. All of these are lesser issues underneath a wearable sensor where evaporation is precluded and where the skin surface would become fully wetted and hydrated. In this paper, a significant focus are the implications for wearable sensors which alleviate rapid sweat evaporation;

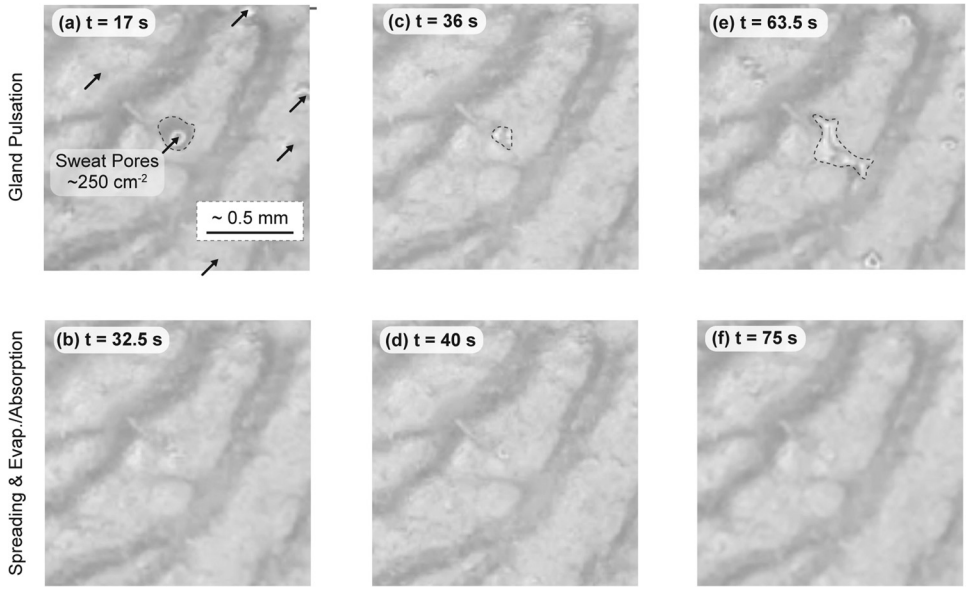

FIG. 3. Images of the finger tip of author Swaile showing individual gland firing, pulsation, and sweat bead recession. The dotted line is the perimeter of the generated sweat.

therefore, when we discuss concentrations of a biomarker, the reader should discard the effects of any concentration increase due to water loss at the skin surface.

To complete this section, the microfluidic flow model can be validated by comparing the sweat gland pressures directly measured in literature,[41] to the resistance flow model provided by Eqs. (1) and (2). Using an experimentally determined flow rate of $Q = 15\ \eta$l/min/gland (Table I) and assuming an average duct diameter of $d = 10\ \mu$m, a pressure of 74 kN/m^2 is calculated which matches the experimental data of Schulz.[41] Additionally, van't Hoff's law can be used to estimate the pressure generated in the gland according to[41]

$$P = \sigma RT\Delta C, \tag{4}$$

where P represents the change in pressure, σ is the osmotic reflection coefficient, R is the gas constant, T is the temperature of the body, and ΔC is the difference in concentration between plasma and sweat often represented in terms of osmolality. Assuming an ideal case with a reflection coefficient of $\sigma = 1$ (complete solute permeability) and an average osmolality difference of 27 mOsm/kg between plasma and sweat,[41] then one determines a hydrostatic pressure capable of 69 kN/m^2. With a model for flow rate of sweat through the eccrine gland now in hand, Sec. IV provides examples of biomarker partitioning into and out of sweat. It will be seen that several of these will exhibit a clear dependency on sweat flow rate.

IV. SWEAT SECRETION AND mM-pM SOLUTE PARTITIONING

Models of biomarker partitioning into sweat are either underdeveloped and/or highly scattered across literature. As stated in the Introduction, development of biosensing technologies for biomarkers in sweat will likely be more successful with a greater appreciation that there are numerous biomarker partitioning mechanisms. This section aims to provide that greater appreciation, to serve as a foundation for those exploring new biomarker opportunities in sweat, and to serve as framework for improved interpretation of previous clinical data. The reader should pay special attention in subsections to whether the biomarker partitioning is said to be sourced from blood, plasma, or serum. Blood is the bodily fluid containing plasma, proteins, red and white blood cells, and a number of solid matters and platelets.[52] Plasma is the fluid of blood containing only proteins, carbohydrates, lipids, and coagulating factors such as fibrin.[52] If these

coagulation factors are removed from plasma one is left with the fluid referred to as serum.[52] Hence, each fluid has a different total solution volume. This greatly affects the discussion of concentration levels and comparisons between studies (i.e., the concentration of a biomarker in blood does not represent the concentration in serum as there is less percentage of blood that is water due to more solids content).

It should also be noted that much of the literature data utilized in this section was obtained using classical clinical techniques, which are crude in comparison to modern wearable methods of sweat sampling.[6–14] Additionally, these previous studies do not benefit from the general modeling framework provided here. Therefore, as the interested reader examines the literature, they should do so with expectation that much improved quality and correlation of data is possible.

This section is organized starting with the smallest sweat solutes (ions) and ending with the largest (proteins). The review begins with the most abundant sweat solutes which form the basis for the sweat generation process itself, sodium and chloride ions. The reader is directed to Table II for a summary of this section.

A. The process of sweat generation, including active partitioning of Na^+ and Cl^- Ions (mM)

The partitioning of Na^+ and Cl^- ions, the most abundant solutes in sweat, is an active process which is also fundamental to the secretion of water. Water and NaCl are partitioned from blood into the lumen of the secretory coil through seven general steps as outlined by several authors:[44,52,53] (1) signals from the brain stimulate cholinergic nerve endings surrounding the sweat gland (due to stress, temperature, or other known stimuli[1,44,54]), (2) stimulation causes Ca^{2+} influx into the surrounding cells, (3) Ca^{2+} stimulates K^+/Cl^- channels causing Cl^- to enter the lumen and K^+ to exit the luminal cells on the basolateral membrane, (4) this exiting of KCl causes a chemical potential gradient permitting co-transport of Na^+-K^+–$2Cl^-$ into the cell, (5) K^+ and Na^+ recycle across the basolateral membrane permitting increased flux of Cl^- into the lumen, (6) once electric field builds, Na^+ enters the lumen via intracellular junctions to re-establish charge neutrality, and (7) the lumen then has greater osmolality (NaCl) than the surrounding cells which causes an influx of water into the lumen to re-equillibrate. This *preliminary* fluid then "pumps" along the length of the duct.

TABLE II. Typical concentration ranges for common biomarkers in sweat versus blood, plasma, and/or serum with subscripts indicating particular fluid (b—blood; p—plasma; s—serum). Please see appropriate sections for all references related to each biomarker.

Biomarker	Partitioning and sweat rate dependent (SWD) or mainly independent (SWI)	Concentration range (mM) in sweat at surface	Concentration range (mM) in blood, plasma, serum	References
Sodium (Na^+)	Active—SWD	10–100	$135–150_p$	55, 88
Chloride (Cl^-)	Active—SWD	10–100	$96–106_s$	55, 89
Potassium ($K^{+)}$	Passive—SWI	4–24	5–6	1, 2, 90
Ammonium (NH_4^+)	Passive (amplified)—SWI	0.5–8	$20–50\times <$ sweat concentration$_p$	1
Ethanol	Passive—SWI	2.5–22.5	$\sim 2.5–22.5_b$	67
Cortisol	Passive—likely SWI	2.21×10^{-5} $–3.86 \times 10^{-4}$	1.24×10^{-4} $–4.0 \times 10^{-4}{}_b$	32, 69, 72
Urea	Various, not confirmed	2–6	$5–7_s$	1, 2, 76, 77
Lactate	Generated by gland—SWD	5–60	$1–7_b$	23, 25, 78, 91
Neuropeptide Y (NPY)	Various, not confirmed	1.88×10^{-10} $–6.82 \times 10^{-10}$	1.41×10^{-10} $–6.11 \times 10^{-10}{}_p$	83
Interleukin 6 (IL-6)	Various, not confirmed	2.91×10^{-10} $–6.54 \times 10^{-10}$	2.15×10^{-10} $–5.69 \times 10^{-10}{}_p$	80, 83

Now, through evolution the body has developed mechanisms to retain electrolytes which would be rapidly lost when large volumes of sweat are used for cooling the body. Once the *preliminary* sweat in the coil is formed, the osmotically generated pressure forces the fluid up from the coil into the ductal region.[1] Sodium and chloride ions are then actively reabsorbed via two channels, the epithelial sodium channel (ENaC) and the CF transmembrane regulator (CFTR), respectively.[52] Levels of both Na^+ and Cl^- are elevated at high sweat rates (Figure 4(b)), indicating that the two channels that reabsorb sodium and chloride ions work at-or-near the same rates regardless of the sweat flow rate in the duct.[52,53] In most instances, chloride concentrations are 20–25 mM less than sodium concentrations due to the contribution of other anions[2] present in sweat such as bicarbonate (HCO_3^-). Both sweat rates and Na^+ and Cl^- concentrations differ across the body due to regional differences in the glands themselves.[55]

A diagrammatic model is presented in Figure 4(a) for the processes of sweat generation, flow (Q) and ductal re-capture of Na^+ and Cl^-. In each instance, the subscript represents the solute of interest, the superscript represents the region of interest (either secretory coil s, duct d, or plasma p) and the superscript asterisk specifically indicates an active transport mechanism. As explained previously, one of the first active transporter mechanisms to respond is chloride channels where the chloride flux in the coil is represented in this model by $*\varphi^s_{Cl}$. Further, the sodium flux into the lumen, as a result of intracellular transport, is represented by φ^s_{Na} where this flux is proportional (ζ) to the chloride flux as a result of the electric field which is created between the lumen and cells. Further, the source of fluid flow Q_{H2O} is directly proportional to the osmotic gradient Π between the lumen of the secretory coil and plasma as a function of the change in concentration $C^s_{Na,Cl} - C^p_{Na,Cl}$, and inversely proportional to the membrane fluid resistance R_m. Regarding the ductal reabsorption of sodium and chloride, the notation takes a similar form as described prior. The reabsorption flux is inversely related to sweat flow rate (Q) as demonstrated in the experimental data[2] of Figure 4(b). A more exhaustive and mathematically predictive model for Na^+ and Cl^- concentration vs. flow rate and position in the duct is provided in Sec. IV B.

B. A microfluidic model for Na^+ and Cl^- concentration vs. sweat rate

Measuring Na^+ and Cl^- in sweat provides limited correlations with concentrations or conditions in blood. There is some evidence that Cl^- levels in sweat can be utilized to predict hormonal changes and therefore ovulation,[56] but such correlations are more likely just a measure of how hormone levels can effect sweat response to external stimuli (e.g., stronger sweat response = higher sweat rate = higher Cl^- concentration). However, there are two unequivocally

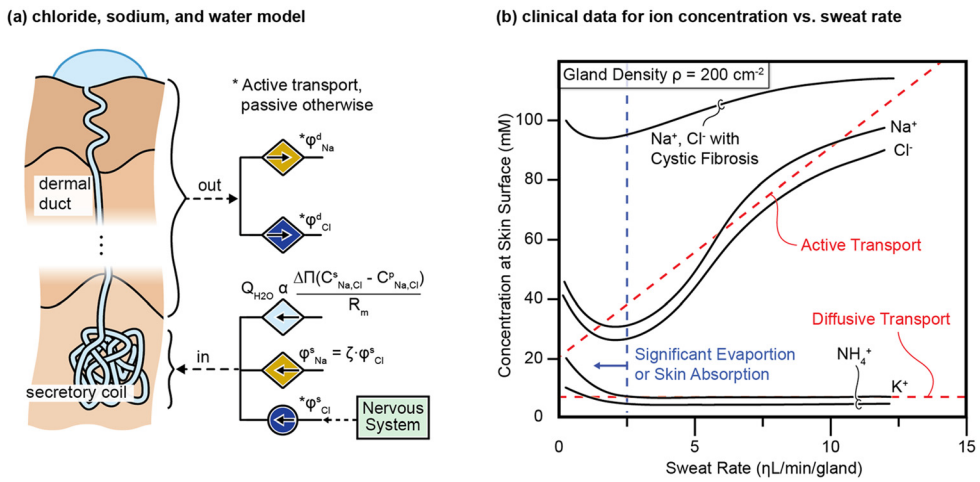

FIG. 4. Transport model for two common electrolytes. (a) Illustrative transport model for sodium, chloride, and water in the eccrine gland. (b) Biomarker surface concentration dependence upon sweat rate, in part adapted from Ref. 2. It is speculated that increased solute concentrations at very low sweat rates are due to evaporation and fluid absorption on the skin.

important uses for monitoring Na^+ or Cl^- in sweat. First, the currently most successful sweat diagnostic product, the Wescor macroduct system, relies exactly on the active nature of reabsorption of Na^+ and Cl^- for cystic fibrosis diagnosis. In cystic fibrosis patients, the cystic fibrosis transmembrane regulator channel does not function properly, wreaking havoc on the body and is evident via increased sweat chloride concentrations.[52] As shown in Figure 4(b), cystic fibrosis is therefore easily non-invasively detected by testing the sweat for higher Cl^- concentration.

The second reason why it is valuable to measure Na^+ and Cl^- in sweat is because the concentrations can be used as an indirect measure of sweat rate utilizing the trends shown in Figure 4(b). Measuring sweat rate is important for improved measures of biomarkers whose concentrations are sweat rate dependent (see Table II) and is important for measuring the effective sampling interval for biomarkers (see Sec. V). To predict sweat rate, Na^+ or Cl^- can be directly measured using ion-selective electrodes[6,7] or electrical conductivity of the sweat can be measured, since Na^+ and Cl^- are the dominantly abundant ions in sweat. Sweat rate or sweat incidence tests based on skin electrical impedance[16,17,19,20] are appearing increasingly in wearable electronics and also rely on measuring the electrical conductivity of sweat. The stratum corneum is highly electrically resistive and therefore a sweat duct filled with salty sweat provides the lowest electrical resistance pathway into the body. Therefore, with more predictive models, quantitative sweat rate measurement can be enabled (beyond the scope of this work) by combining: the geometrical model of Figure 1 and Table I; the concentration data of Figure 4; and an even more detailed concentration model which is now presented in detail.

Clearly, a thorough model of Na^+ and Cl^- concentration vs. sweat rate would be beneficial to sweat biosensing. Furthermore, a model should provide a spatial concentration profile of Na^+ and Cl^- in the duct, which could have impact on impedance measurements of sweat rate and possibly the partitioning of some other solutes into sweat (speculation). Therefore, building on the flow rate (Q) model of previous sections, a predictive model is provided for the profile of Na^+ and Cl^- concentration along the duct and at the surface of skin. The lengthy derivation of this model is provided in Appendix A,[92] and the final result is

$$C(z) = C_s \cdot e^{-\frac{2k\pi R}{Q}[z+L]}, \tag{5}$$

where $C(z)$ is the concentration of the solute as a function along the length of the duct L with the surface being $z = 0$, C_s is the concentration of the solute in the preliminary sweat (secretory coil), k is the reabsorption permeability constant of the solute in the sweat duct, R is the radius of the duct, and Q is the volumetric flow rate. Equation (5) assumes that radial diffusion can be neglected, the fluid (sweat) is well-mixed, the interstitial fluid concentration C_{if} is equal to zero and that the solute transport into the lumen is proportional to the concentration gradient from the lumen to interstitial fluid.

Equation (5) can be further utilized to predict the Na^+ and Cl^- concentrations of emerging sweat vs. flow rate in a more accurate fashion than that of the linear estimate (red dotted line) of Figure 4(b). At very high flow rates of sweat, the experimental non-linear relationship could be limited by diffusion of Na^+ and Cl^- to the reabsorption walls of the duct (neglected in Appendix A[92] and Eq. (5)) and/or due to a limited rate of active reabsorption. At very low sweat rates, the increase seen for all sweat solutes in Figure 4(b) is possibly due to the effects of evaporation and/or water absorption into the skin (speculation, as sample was not measured as it emerged from the sweat gland). Such speculation is further supported by decades of sweat rate measurements by skin conductance, where a wearable sensor is placed over skin and prevents evaporation, which provides a real time measurement of Na^+ and Cl^- concentration in the duct and importantly for which there is clearly no inflection point in plots of skin conductance vs. increasing sweat rate.[17,19] Therefore, if the data in Figure 4(b) were re-measured with a wearable electronic device (hydrated skin with no evaporation), it is speculated that the concentration increase observed at low sweat rates might not appear.

C. Passive ion partitioning: Potassium (mM)

Potassium partitioning is interesting to examine because although it is a small ion like sodium or chloride, its transport mechanism is vastly different. From an applied perspective, K^+ in plasma predicts muscle activity[57] and a myriad of conditions related to hypo- or hyperkalemia.[58] Further, K^+ concentration in sweat is proportional to blood concentration and is independent of sweat rate.[59] The precise method of K^+ partitioning into sweat has not been fully confirmed but the concentration appearing at the surface of skin is likely influenced by K^+ leak channels in the duct[44] (Figure 5(a)). Sato[1] conducted a very detailed analysis of measuring K^+ exiting the secretory coil vs. K^+ exciting the duct onto the surface of skin. The results for the preliminary sweat emerging from the secretory coil showed K^+ isotonic to blood (~5 mM). However, sweat emerging from the duct was found to be several mM higher in concentration, possibly indicating that the active process of ductal reabsorption of Na^+ results in possible secretion of K^+ into sweat in the duct. Sato's experiment was conducted on glands extracted from the palm (not in the body). An invariance of K^+ with sweat rate and ~5 mM concentrations have also been shown with true human subjects testing by Patterson.[55]

D. Weak acid or base partitioning which is passive but amplified or suppressed: Ammonia (mM)

Ammonia is of interest in sweat because it has been shown to track with exercise intensity and blood levels.[24,61,62] Ammonia is also of interest because it is a possible and needed substitute for lactate measurement of anaerobic condition (see Subsection IV H). Ammonia (NH_3) passes through the cells lining the secretory coil by means of a passive diffusive mechanism.[1] In the lumen, most ammonia molecules that partition from blood will protonate to ammonium (NH_4^+) due to the relatively low pH of sweat which approaches a pH of 5 for low sweat rates and increases towards 7 at higher sweat rates.[2] Assuming an ammonia pKa of 9.3, the Henderson-Hasselbalch equation then predicts that even at a pH of 7, the vast majority of ammonia (NH_3) that is able to diffuse into the sweat gland lumen will be protonated in sweat into ammonium[63] (NH_4^+). Therefore, while NH_3 has a high level of diffusivity through cellular membranes, NH_4^+ will not because of its electrical charge.[2] This essentially causes "trapping" of ammonium in the lumen of the secretory coil and dermal duct. This supports the discovery that the concentration of ammonium (NH_4^+) in sweat is *amplified* (20–50 times higher) compared to the concentration of ammonium in plasma.[1] The effective amplification coefficient (pH dependence) of ammonium concentration in sweat is represented as $\gamma(pH)$ in Figure 5(a). Note, in this instance, $\gamma(pH)$ is a factor which depends on the rate of plasma ammonia ($C_{NH_3,plasma}$)

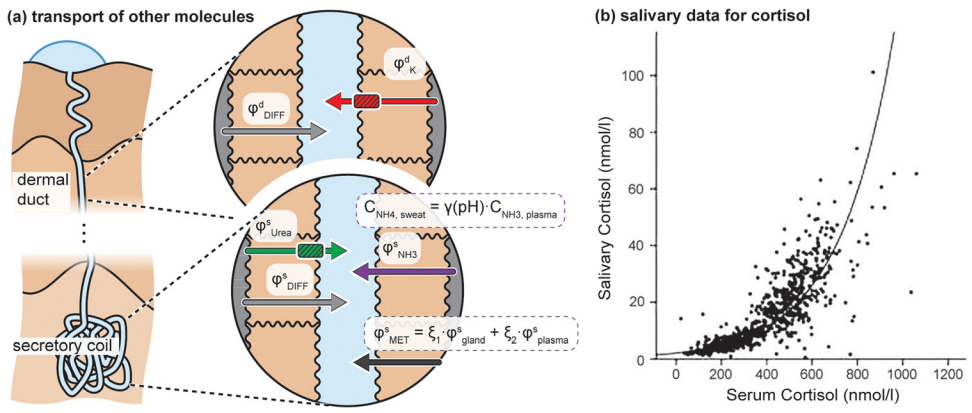

FIG. 5. Transport of molecules other than sodium or chloride. (a) Illustrative partitioning model for potassium, ammonia, urea, molecules of metabolic origin, and a placeholder for other diffusively partitioning biomarkers. (b) Relationship between salivary and serum cortisol. Reprinted with permission from Hellhammer *et al.*, "Salivary cortisol as a biomarker in stress research," Psychoneuroendocrinology **34**, 163–171 (2009). Copyright 2009 Elsevier.[60]

diffusion and sweat flow rate Q. More details can be found elsewhere.[23,61,62,64] Regardless, this protonation of ammonia is practically beneficial as it increases the concentration, which potentially simplifies sensor detection methods.[10]

Ammonia is one example of many possible examples of molecules which could permeate the epithelial membrane of the eccrine sweat gland via diffusion and become entrapped within the lumen due to ionization. This statement holds true for most *weak bases*. However, sweat would have to reach an alkaline pH level (7–9 pH) before any appreciable trapping of ionized *weak acid* species would occur as a result of deprotonization. This pH dependence also raises an element of caution for researchers measuring weak acid or weak bases in sweat. If the sweat is not rapidly measured or collected and sealed, carbon-dioxide in the atmosphere could be absorbed into and dissociate in sweat to make it more acidic. This could change, for example, the concentrations and sensing therefore of protonated vs. a non-protonated solute.[65]

E. Passive small molecule partitioning: Ethanol (alcohol, mM)

Ethanol metabolism is well-studied in humans as it is the key molecule which causes intoxication via excessive consumption of alcohol. Several studies show a strong correlation between blood and sweat ethanol concentrations which could potentially enable continuous blood-alcohol (BAC) analysis by sweat measurement.[66–68] Gamella *et al.* presented a non-invasive electrochemical bio-sensing device which monitored ethanol concentrations in sweat whilst demonstrating higher sensitivity compared to breathalyzers commercially available at the time (2014).[66] Furthermore, their device showed a response to sweat ethanol concentrations within only 5 min after ingestion of an alcoholic beverage, while also demonstrating strong correlation to BAC ($r = 0.934$).[66] Such capability is available commercially (e.g., a wearable bracelet by SCRAM® Systems).

Due to the hydrophilic-lipophilic balanced nature of ethanol, this molecule is water-soluble and has the ability to permeate through most membranes within the human body. In many studies on ethanol concentration, correlations between sweat and blood conclude that ethanol is found about 20% more concentrated in sweat compared to blood or plasma.[66,68] However, when comparing the water contents of blood and sweat, one also finds that sweat has approximately 20% more water than that of blood.[67] In fact, when comparing the concentration of ethanol in terms of milli-moles per liter of water instead of liter of solution (more generalized), one finds that sweat and blood ethanol concentrations correlate one to one.[67] This simple result further shows that numerous types of alcohols likely correlate well between sweat and blood. Furthermore, this reinforces that correlations with blood should always consider the fact that blood has a lesser percentage of water compared to sweat.

F. Passive small molecule partitioning: Cortisol (ηM)

Cortisol is a vital life hormone released in response to stress from the hypothalamo-pituitary-adrenal axis.[69] Cortisol's lipid-soluble nature allows for passive transport between the lipid-bilayer membrane of cells, allowing for cortisol's presence to be detected in many bodily fluids including sweat.[70] However, there are two distinct structures of cortisol. Namely, unbound cortisol which is able to diffuse through membranes via intracellular passive transport, while cortisol bound to carrier proteins is unable to make this diffusion.[32,70] In saliva, free cortisol is carried by the bloodstream to acinar cells at the ends of the salivary glands where its lipid-soluble nature allows for passive transport into the salivary glands, causing salivary cortisol levels to be independent of salivary rates.[71] Studies also show that saliva cortisol correlates with serum unbound cortisol levels[32] (Figure 5(b)).

This mechanism of unbound cortisol partitioning and salivary rate independence found in salivary gland function can be speculated to be true for sweat glands as well. Figure 5(a) illustrates generic examples of passive coil and ductal diffusion of solutes with φ^{s}_{DIFF} and φ^{d}_{DIFF} representing the diffusional flux from the secretory coil and dermal duct, respectively. Cortisol levels in sweat have been recorded as ranging from $\sim 2.21 \times 10^{-5}$ to 3.86×10^{-4} mM, with the greatest concentration being found in the morning and correlating with salivary

concentrations.[69] Comparatively, blood cortisol concentrations typically range from $\sim 1.24 \times 10^{-4}$ to 4.0×10^{-4} mM.[72] It should be noted that type 2 11-β-hydroxysteroid-dehydrogenase (HSD), which is an enzyme capable of converting cortisol to cortisone, has also been detected in cells of the eccrine sweat gland duct.[72]

G. Active small molecule partitioning: Urea (mM)

Urea is a nitrogen-containing metabolite typically excreted by the kidney but is found to be alternatively excreted through sweat glands. Urea from sweat is even visibly observable as a white skin crust in patients suffering from kidney failure[73,74] (with urea levels up to 50 times greater than in serum[74]). Urea partitioning into sweat has not been fully confirmed but ideas of passive transport across glands from blood into sweat precursor fluid has been a common speculation[1,2,75,76] and emphasized by urea's diffusibility through membranes as well as its ratio relationships to plasma.[76] Another theory of urea partitioning is possible metabolism by the sweat glands[1,2] or other means such as Urea Transporter-B (UT-B).[73,74,77] Regardless, urea concentrations in sweat for healthy males is typically in the range[2,76] from 2 to 6 mM, with serum urea concentrations ranging from $\sim$5 to 7 mM.[77] At low sweat rates, the sweat to plasma urea concentration ratio reaches upper limits of 4 but approach 1 as sweat rates increase.[1,75,76] Other studies are less conclusive, perhaps due to use of significantly uncontrolled sweat generation and collection methods.[77] Further study is clearly needed to determine if clinical data with higher urea concentration at low sweat rates is due to evaporation or other causes.

H. Small molecules generated by the gland: Lactate (mM)

Lactate is a small molecule metabolite produced by the body as a result of anaerobic activity (high exertion exercise, critically ill patients, etc.).[64] Lactate is used to sustain the purine nucleotide cycle (PNC) and tricarboxylic acid cycle (TCA cycle) which allows energy production in the absence of adequate oxygen.[64] The transport of lactate from plasma to sweat remains not fully understood and inherently complex. Lactate partitioning, and possibly partitioning of other metabolites as well, is represented in the secretory coil of Figure 5(a) as φ^s_{MET}. As shown in Figure 5(a), φ^s_{MET} has two likely origins: (1) a flux of the metabolite due to the metabolism of a "hard-working" sweat gland itself φ^s_{gland} and (2) any active or passive transport mechanism which transports the metabolite between plasma and sweat φ^s_{plasma}. Further, the flux generated will likely have proportionality constants as shown ξ_1 and ξ_2, and ξ_2 could be negative in value if ξ_1 is sufficient to create a higher concentration of lactate in sweat than in plasma (diffuse back into plasma). Such a concentration gradient in either direction could also cause diffusive transport in the duct.

What is clear at this point is that sweat lactate is at least an indirect indicator of body exertion[11] and is likely more directly related exertion of the sweat gland itself in response to whole body exertion. Several studies[24,25,78] have experimentally investigated the relationship between plasma and sweat lactate levels *after* exercise, with widely ranging sweat concentrations as low[24] as $\sim$6 mM and as high[21] as $\sim$100 mM.

I. Peptides and small protein partitioning: Neuropeptides and cytokines (pM)

Various peptides and small proteins have been detected in eccrine sweat and have been shown to correlate with plasma levels. Polypeptides are long linear chains of multiple amino acids found throughout the body.[79] Proteins are also chains of amino acids and therefore can be classified as polypeptides, but are typically seen as three-dimensional structures rather than in linear form.[79] This section deals with two subsets of proteins and peptides: cytokines and neuropeptides. These structures are much larger than small molecules and their partitioning into sweat is unexpected at first glance. Exact partitioning models remain unknown, but the initial work on sweat correlations with blood is promising and therefore briefly reviewed here.

Cytokines are reduced regulatory proteins synthesized and released by immune system cells as well as a variety of other cells including those in eccrine sweat glands.[80] In previous sweat

patch studies, interleukin-6 (IL-6), IL-1α, IL-1β, IL-8, tumor necrosis factor-α (TNF-α), and transforming growth factor-β (TGF-β) have been detected directly in eccrine sweat and have been shown to have a direct correlation with plasma levels.[80] However, cytokines can also be reproduced systemically or locally[80] at the sweat gland. Many cytokine responses are systemic in cytokine production, such that cytokine production by or near the sweat gland would mirror cytokine production in the body, such that sweat gland produced cytokines could still correlate with concentrations in blood. Therefore, in some cases, the "source" of the cytokine generation may be less important.

Peptides such as neuropeptide Y (NPY) also display correlation between sweat and blood. NPY is a linear polypeptide found in dermal nerve fibers, sweat glands, and hair follicles.[81] NPY is found to exhibit anti-stress activities when receptors are activated, along with numerous other effects such as anti-depressive properties.[82] In a study of women with major depressive disorder (MDD) in remission, levels of cytokine and neuropeptide concentrations were measured via sweat patch and plasma comparisons.[83] It was displayed that levels of sympathetic NPY increased from 4.45×10^{-10} mM in sweat of healthy patients to 1.19×10^{-8} mM in sweat of MDD patients, with levels comparable to plasma concentrations in both groups.[83] This is presumably due to an elevation in stress response due to MDD.

The reader should carefully note, however, that the above reviewed studies are for *sweat patches* worn for 24 h. Such patches will collect a significant amount of sweat generated at very low flow rates, flow rates low enough that even peptides and proteins have adequate time to diffuse into similar concentrations in sweat and plasma. It therefore remains to be seen if peptides and small protein concentrations in sweat have a significant dependence on sweat rate. It is fully expected that their concentrations will decrease substantially at high sweat rates, given their large size which generally reduces both solute diffusivity and membrane permeability.

V. IMPLICATIONS FOR BIOSENSING SAMPLING INTERVALS

With a microfluidic model for the eccrine now in hand, along with a greater understanding of the various mechanisms through which biomarkers partition into sweat, implications on external sensing of sweat can now be considered, i.e., at what rate or sampling interval can biomarkers in blood (*in-vivo*) be correlated with sensing of sweat external to the skin (*ex-vivo*)?

A. Speed of partitioning into sweat: General evidence

Some assumptions must first be made on the rates at which biomarkers partition into sweat. Two forms of evidence are presented that support that the partitioning rate is as fast as or faster than several minutes. First, many sweat solutes such as K^+, NH_4^+, urea, and ethanol exhibit sweat concentrations that are only weakly inversely proportional to sweat rate or even independent of sweat rate. Therefore, their partitioning is rapid enough that their transport to the skin surface is primarily sweat flow rate Q limited and not partitioning-rate limited. Consider the case of a 4 ηl/min/gland sweat rate and a maximum volume per gland of 8 ηl (Table I). In this example, the sweat in the gland is refreshed no slower than every 2 min, implying that biomarker partitioning is at least that fast. For solutes like K^+, it is clearly much faster, considering gland volumes can be <1 ηl (Table I) and K^+ is fairly invariant with sweat rate. This observation could be practically important as K^+ in blood has been shown to correlate rather quickly with muscle activity;[57] however, other temporal challenges may remain as will be discussed in Sec. V B. Next, consider also the experimental evidence of Hurley, where fluorescein dye (m.w. 332 g/mol) was administered intravenously.[84] In this study, fluorescence was observed in the lips and other extremities within 20 s after injection (circulation time) and fluorescence appeared in sweat on the skin surface 2 min after injection of fluorescein. Therefore, it is clear that many blood solutes partition into sweat in a matter of minutes and in many cases much faster. Practically, for many small-size solutes, their partitioning is therefore effectively "real time" in the context of "continuous" physiological monitoring

Possible exceptions to fast partitioning could be larger solutes such as proteins or peptides, but these same larger solutes often systematically partition into blood at slower rates for the same reasons they might more slowly partition into sweat. Furthermore, many protein and peptide concentration changes due to physiological responses to stimuli are inherently slow as well. Therefore, many large solutes which slowly partition into sweat may still effectively represent "real time" biosensing in the context of "continuous" physiological monitoring. However, these slowly partitioning solutes will need to be sampled at low sweat rates, or at higher sweat rates they will need to be concentration corrected with co-measurement of sweat rate per gland.

B. Rationale for bringing sensors to the eccrine glands

If many biomarkers from blood partition quickly into sweat, then the remaining bottlenecks in sampling interval are: (1) how quickly biomarkers transport to the sensor and (2) how long it requires for the sensor to respond, especially for pM concentrations where solute concentrations near the sensor could be depleted during sensor capture. The answer for the latter varies extremely widely across specific examples, but generally, numerous sensing modalities can support minute-level sampling intervals. The former, microfluidic transport to the sensor itself, is more relevant to this paper and has a significant effect on the sampling intervals. The vast majority of sweat biosensing in the literature involves manual collection bags or textiles, or in more advanced studies microfluidic components which wick sweat past wearable sensors. Here, a model will focus on bringing sensors directly to the skin[6–14] which provides several advantages: (1) reading of a change in biomarker concentration is more immediate and (2) there is less time for sample degradation or contamination. Generally, this also reduces the complexity of the sensing device, but requires diligence in development of sensors which do not require sample pretreatment or solute introductions such as redox mediators.[85]

C. Expectations for biomarker sampling intervals

As shown in Figure 6, a microfluidic model for sampling interval considers the case of a sensor brought into close proximity with skin. Derivations and assumptions for the model are provided with the supplementary material in Appendix B.[92] The model is informative, but simplified and is not a replacement for more sophisticated simulations or real *in-vivo* characterization. Limitations and caveats of the model will be discussed at the end of this section.

Plotted in Figure 6(b) are sampling times (τ_{sample}) for filling the volume under the sensor with new sweat fluid vs. sweat flow rate from each gland. The plot uses equations derived in Appendix B[92] for a cylindrical coordinate system, for a 2.5 mm diameter sensor, with a 30 μm effective gap from skin (includes volume of skin grooves[86,87]) and a sweat gland density of 140 glands/cm^2 (the abdomen). The data in Figure 6(b) does not take into effect fluid mixing, fluid boundary layer with the sensor, or diffusion. There is an upper and lower range for sampling time bounded by two extremes, for which the real case is somewhere in between. The best-case limit is the "single-centered" case, which assumes all sweat is introduced at the radial center of the sensor. The "single-centered" case is easily calculated as how long is required for a flow rate of new sweat (Q_{TOT}) to displace the entire volume V_{TOT} of older sweat between the sensor and the skin ($\tau_{sample} = V_{TOT}/Q_{TOT}$). The worst-case limit is based on a homogenous distribution of sweat generation underneath the sensor (i.e., glands everywhere) and time it would take one unit of sweat to travel from $0.05 \cdot R$ units from the center of the sensor to the edge radius R. ($\tau_{sample} = \int_{0.05 \cdot R}^{R} v_{flow}^{-1} \cdot dr$, see Appendix B[92] for assumptions and derivation related to v_{flow}). Obviously, in a real sensing application, 100% of new sweat sample is not required for meaningful measurement of a change in biomarker concentration, so the actual sampling time could be less, as plotted as "66% Refill" for each case in Figure 6(b). The plot in Figure 6(b) clearly shows that sampling times of "*new fluid*" are possible in the range of 4–25 min for a sweat generation rate of 5 ηl/min/gland. If the sensor can be brought closer to the skin, and/or a filler material can be provided in the gap between sensor or skin, and/or smaller sensor radii

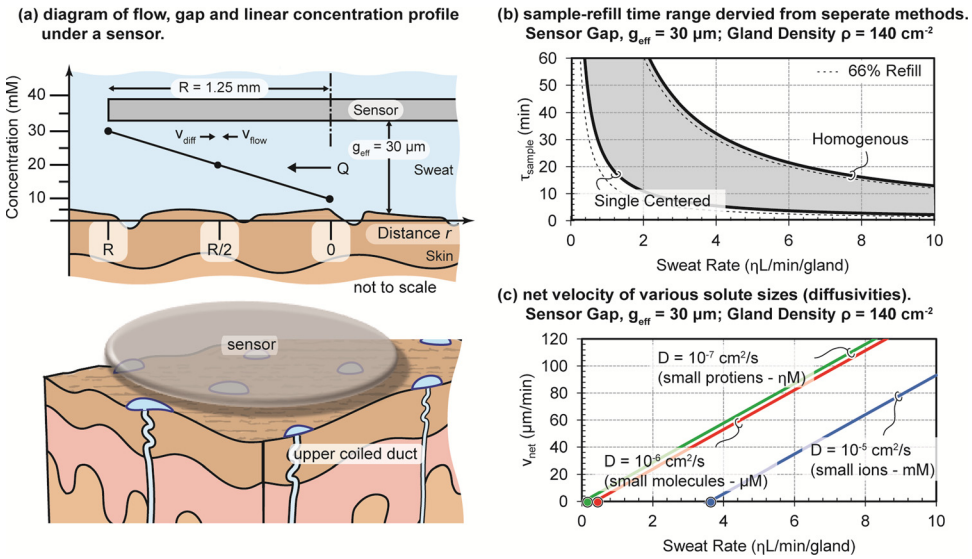

FIG. 6. Estimation of the minimum sampling time (refresh rate) for a sweat biosensor. (a) Representation of the case where there is a linear concentration gradient below the sensor with flow (v_{flow}) and diffusional (v_{diff}) velocities in opposition. (b) The effective refill time from two separate derivation methods, see Appendix B in the supplementary material.[92] (c) Simple, net molecular velocity underneath the sensor. Please see Appendix B[92] for a full derivation.[86,87]

can be implemented, these sampling times can be significantly reduced proportional to the reduction in volume.

Sampling time, however, is not necessarily the predictor of chronological resolution for sweat biosensing, i.e., can a rapid change in biomarkers partitioned into sweat result in delayed but otherwise fully proportional change in sensor reading as those biomarkers reach the sensor? One reason it will not is because of solute diffusion. The diagram in Figure 6(a) assumes that outside the sensor the concentration is higher (older sweat) at 30 mM of a small ion, and the newly emerging sweat is 10 mM, with a simple linear concentration dependence in between. For this case, the solute will diffuse back towards the center of the sensor, confounding the measurement, with an average diffusional velocity along this sensor radius estimated according to a modified Fick's first law

$$\bar{v}_{diff}|_0^R = \frac{D}{R}\ln\left[\frac{\Delta C + C(0)}{C(0)}\right], \tag{6}$$

where $\bar{v}_{diff}$ is the average diffusional velocity from zero to R, D is the diffusivity of the analyte, R is the full radius of the sensor, ΔC is the concentration difference from zero to R, and $C(0)$ is the concentration at $r = 0$.

In this model, average fluid velocity (advective) over the same region is determined to be

$$\bar{v}_{flow}|_0^R = \frac{Q \cdot \rho \cdot R}{4 g_{eff}}, \tag{7}$$

where $\bar{v}_{flow}$ is the average flow velocity from zero to R, Q is the sweat flow rate per gland, ρ is the density of sweat glands underneath the sensor region, R is the radius of the sensor, and g_{eff} is the effective gap height as a result of sensor to skin spacing and grooves of the skin. The point of concern is when diffusion velocity (Eq. (6)) dominates over advective fluid velocity (Eq. (7)). This is presented in Figure 6(c) using the same parameters used for Figure 6(b), and for three general classes of solutes in sweat with significantly different diffusivities and concentrations in sweat (mM small ions, μM small molecules, and ηM small proteins). If the net velocity ($\bar{v}_{flow} - \bar{v}_{diff}$) is below zero then due to back-diffusion of solutes there will be a

significant broadening of the chronological resolution of sweat biosensing. For the example sensor radius used here (1.25 mm) and linearly graded concentration profile presented, it appears that the small ions can be of concern at low sweat generation rates, but that diffusion will play an insignificant role for small molecules and proteins except for very low sweat generation rates (<0.5 ηl/min/gland).

The reader is cautioned that models used for Figure 6 and in Appendix B[92] only reveal that in some cases advective flow rate and diffusion are non-issues for rapid biomarker sampling. In other cases, diffusion into or out of contamination sources such as dead surface skin cells will more significantly confound the measurement. Also, fluid boundary layers at the sensor surface and turbulent flow and mixing could be the real limiters of chronological resolution. Regardless, these models do provide a more complete picture of the microfluidics and biomarker transport from blood all the way to sensor, and demonstrate that effectively real-time biosensing is plausible for numerous biomarkers and applications.

D. Brief arguments for sweat biosensing compared to other non-invasive biofluids

There are numerous arguments that could be presented for or against use of any biofluid for biomarker sampling, but here the discussion is limited to only those arguments that relate directly to the findings of this paper. There are several insights that favor using sweat as a non-invasive biofluid compared to other possible non-invasive biofluids (saliva, tears, and urine). First, the previous section highlighted the issue of old and new sweat samples (and solutes) mixing and confounding the measurement. Compared to other non-invasive biofluids, sweat biosensing may have a unique advantage in bringing sensors into closest proximity with the biofluid as it is created. Furthermore, sweat can potentially do this in a manner that in many aspects is more convenient and ergonomic to the human subject being tested. Second, if the fluidic volume between the sensor and the sweat gland can be adequately minimized to allow sensing at low sweat rates, another advantage of sweat could be a wider-range of biomarkers that correlate with blood. Specifically, sweat is unique in that it can likely be continually sampled at low fluid generation rates without physiological consequence to the human subject (e.g., dry mouth or dry eyes). Low fluid generation rates might allow biomarkers which have low membrane permeability (due to size or low lipophilicity) to have adequate time to partition into the biofluid such that maximum correlation with blood is possible. Otherwise, such biomarkers could be diluted at moderate to high bio-fluid generation rates. The above two arguments are of course highly dependent on each exact usage and biomarker case, but this paper provides the general constructs of how to further explore biomarker opportunities in sweat and compare them with other possible biofluid sampling methods.

ACKNOWLEDGMENTS

The authors would like to acknowledge support from the National Science Foundation and the industrial members of the Center for Advanced Design and Manufacturing of Integrated Microfluidics (NSF I/UCRC Award No. IIP-1362165) and the Air Force Office of Scientific Research: Summer Faculty Fellowship Program. Further, special acknowledgement is made to the numerous scientific contributions and inspiring work of K. Sato and colleagues.[1]

[1]K. Sato *Reviews of Physiology, Biochemistry and Pharmacology* (Springer, 1977), Vol. 79, pp. 51–131.
[2]K. Sato, W. H. Kang, K. Saga, and K. T. Sato, "Biology of sweat glands and their disorders. I. Normal sweat gland function," J. Am. Acad. Dermatol. **20**, 537–563 (1989).
[3]N. De Giovanni and N. Fucci, "The current status of sweat testing for drugs of abuse: A review," Curr. Med. Chem. **20**, 545–561 (2013).
[4]D. A. Kidwell, J. C. Holland, and S. Athanaselis, "Testing for drugs of abuse in saliva and sweat," J. Chromatogr. B **713**, 111–135 (1998).
[5]A. Mena-Bravo and M. D. Luque de Castro, "Sweat: A sample with limited present applications and promising future in metabolomics," J. Pharm. Biomed. Anal. **90**, 139–147 (2014).
[6]D. P. Rose *et al.*, "Adhesive RFID sensor patch for monitoring of sweat electrolytes," IEEE Trans. Biomed. Eng. (published online).
[7]A. J. Bandodkar *et al.*, "Epidermal tattoo potentiometric sodium sensors with wireless signal transduction for continuous non-invasive sweat monitoring," Biosens. Bioelectron. **54**, 603–609 (2014).

[8]A. J. Bandodkar and J. Wang, "Non-invasive wearable electrochemical sensors: A review," Trends Biotechnol. **32**, 363–371 (2014).
[9]A. J. Bandodkar *et al.*, "Tattoo-based noninvasive glucose monitoring: A proof-of-concept study," Anal. Chem. **87**, 394–398 (2015).
[10]T. Guinovart, A. J. Bandodkar, J. R. Windmiller, F. J. Andrade, and J. Wang, "A potentiometric tattoo sensor for monitoring ammonium in sweat," Analyst **138**, 7031–7038 (2013).
[11]W. Jia *et al.*, "Electrochemical tattoo biosensors for real-time noninvasive lactate monitoring in human perspiration," Anal. Chem. **85**, 6553–6560 (2013).
[12]W. Jia *et al.*, "Wearable textile biofuel cells for powering electronics," J. Mater. Chem. A **2**, 18184–18189 (2014).
[13]J. Kim *et al.*, "Wearable temporary tattoo sensor for real-time trace-metal monitoring in human sweat," Electrochem. Commun. **51**, 41–45 (2015).
[14]T. Guinovart, G. Valdés-Ramírez, J. R. Windmiller, F. J. Andrade, and J. Wang, "Bandage-based wearable potentiometric sensor for monitoring wound pH," Electroanalysis **26**, 1345–1353 (2014).
[15]A. Luchini *et al.*, "Nanoparticle technology: Addressing the fundamental roadblocks to protein biomarker discovery," Curr. Mol. Med. **10**, 133–141 (2010).
[16]S. Grimnes, A. Jabbari, Ø. G. Martinsen, and C. Tronstad, "Electrodermal activity by DC potential and AC conductance measured simultaneously at the same skin site," Skin Res. Technol. **17**, 26–34 (2011).
[17]C. Tronstad, S. Grimnes, Ø. G. Martinsen, and E. Fosse, in *13th International Conference on Electrical Bioimpedance and the 8th Conference on Electrical Impedance Tomography, Vol. 17 IFMBE Proceedings*, edited by H. Scharfetter and R. Merwa (Springer Berlin Heidelberg, 2007), Chap. 63, pp. 236–239.
[18]C. Tronstad, "Developments in biomedical sensors based on electrical impedance," Doctor Philosophiae thesis (University of Oslo, 2012).
[19]C. Tronstad, H. Kalvøy, S. Grimnes, and Ø. G. Martinsen, "Improved estimation of sweating based on electrical properties of skin," Ann. Biomed. Eng. **41**, 1074–1083 (2013).
[20]C. Tronstad, H. Kalvøy, S. Grimnes, and Ø. G. Martinsen, "Waveform difference between skin conductance and skin potential responses in relation to electrical and evaporative properties of skin," Psychophysiology **50**, 1070–1078 (2013).
[21]L. S. Lamont, "Sweat lactate secretion during exercise in relation to women's aerobic capacity," J. Appl. Physiol. **62**, 194–198 (1987).
[22]S. P. Duvillard, "Exercise lactate levels: Simulation and reality of aerobic and anaerobic metabolism," Eur. J. Appl. Physiol. **86**, 3–5 (2001).
[23]P. J. Derbyshire, H. Barr, F. Davis, and S. P. J. Higson, "Lactate in human sweat: A critical review of research to the present day," J. Physiol. Sci. **62**, 429–440 (2012).
[24]I. Alvear-Ordenes, D. García-López, J. A. De Paz, and J. González-Gallego, "Sweat lactate, ammonia, and urea in rugby players," Int. J. Sports Med. **26**, 632–637 (2005).
[25]J. M. Green, P. A. Bishop, I. H. Muir, J. R. McLester, Jr., and H. E. Heath, "Effects of high and low blood lactate concentrations on sweat lactate response," Int. J. Sports Med. **21**, 556–560 (2000).
[26]M. J. Buono, N. V. L. Lee, and P. W. Miller, "The relationship between exercise intensity and the sweat lactate excretion rate," J. Physiol. Sci. **60**, 103–107 (2010).
[27]J. Moyer, D. Wilson, I. Finkelshtein, B. Wong, and R. Potts, "Correlation between sweat glucose and blood glucose in subjects with diabetes," Diabetes Technol. Ther. **14**, 398–402 (2012).
[28]T. A. Peyser, R. O. Potts, H. L. Berman, J. W. Moyer, and M. A. Kouchnir, "Devices, methods, and kits for non-invasive glucose measurement," U.S. patent 7,725,149 (2010).
[29]Y.-H. Lee and D. T. Wong, "Saliva: An emerging biofluid for early detection of diseases," Am. J. Dent. **22**, 241–248 (2009).
[30]V. Oncescu, D. O'Dell, and D. Erickson, "Smartphone based health accessory for colorimetric detection of biomarkers in sweat and saliva," Lab Chip **13**, 3232–3238 (2013).
[31]T. Pfaffe, J. Cooper-White, P. Beyerlein, K. Kostner, and C. Punyadeera, "Diagnostic potential of saliva: Current state and future applications," Clin. Chem. **57**, 675–687 (2011).
[32]T. Umeda *et al.*, "Use of saliva for monitoring unbound free cortisol levels in serum," Clin. Chim. Acta **110**, 245–253 (1981).
[33]D. Pieragostino *et al.*, "Unraveling the molecular repertoire of tears as a source of biomarkers: Beyond ocular diseases," Proteomics – Clin. Appl. **9**, 169–186 (2015).
[34]R. F. Rushmer, K. J. K. Buettner, J. M. Short, and G. F. Odland, "The skin," Science **154**, 343–348 (1966).
[35]K. Sato and F. Sato, "Individual variations in structure and function of human eccrine sweat gland," Am. J. Physiol. **245**, R203–R208 (1983).
[36]K. Wilke, A. Martin, L. Terstegen, and S. S. Biel, "A short history of sweat gland biology," Int. J. Cosmet. Sci. **29**, 169–179 (2007).
[37]P. U. Giacomoni, T. Mammone, and M. Teri, "Gender-linked differences in human skin," J. Dermatol. Sci. **55**, 144–149 (2009).
[38]K. Saga, "Structure and function of human sweat glands studied with histochemistry and cytochemistry," Prog. Histochem. Cytochem. **37**, 323–386 (2002).
[39]W. C. Randall and C. Calman, "The surface tension of human sweat; its determination and its significance," J. Invest. Dermatol. **23**, 113–118 (1954).
[40]K. Sato, A. Nishiyama, and M. Kobayashi, "Mechanical properties and functions of the myoepithelium in the eccrine sweat gland," Am. J. Physiol. - Cell Physiol. **237**, C177–C184 (1979).
[41]I. J. Schulz, "Micropuncture studies of the sweat formation in cystic fibrosis patients," J. Clin. Invest. **48**, 1470–1477 (1969).
[42]R. G. Hibbs, "The fine structure of human eccrine sweat glands," Am. J. Anat. **103**, 201–217 (1958).
[43]F. Sato, M. Burgers, and K. Sato, "Some characteristics of adrenergic human eccrine sweating," Experientia **30**, 40–41 (1974).
[44]K. Sato, "The mechanism of eccrine sweat secretion," Perspect. Exercise Sci. Sports Med. **6**, 85–118 (1993).

[45]N. A. S. Taylor and C. A. Machado-Moreira, "Regional variations in transepidermal water loss, eccrine sweat gland density, sweat secretion rates and electrolyte composition in resting and exercising humans," Extreme Physiol. Med. **2**, 1–29 (2013).
[46]W. P. Morgan and L. E. Hughes, "The distribution, size and density of the apocrine glands in *Hidradenitis suppuritiva*," Br. J. Surg. **66**, 853–856 (1979).
[47]L. Hou *et al*., "Artificial microfluidic skin for *in vitro* perspiration simulation and testing," Lab Chip **13**, 1868–1875 (2013).
[48]H. Bruus, *Theoretical Microfluidics* (Oxford University Press, 2008), Vol. 18, p. 346.
[49]C. N. Peiss, W. C. Randall, and A. B. Hertzman, "Hydration of the skin and its effect on sweating and evaporative water loss," J. Invest. Dermatol. **26**, 459–470 (1956).
[50]W. C. Randall and C. N. Peiss, "The relationship between skin hydration and the suppression of sweating," J. Invest. Dermatol. **28**, 435–441 (1957).
[51]F. Mugele and J.-C. Baret, "Electrowetting: From basics to applications," J. Phys.: Condens. Matter **17**, R705–R774 (2005).
[52]W. F. Boron and E. L. Boulpaep, *Medical Physiology: A Cellular and Molecular Approach*, 2nd ed. (Elsevier Health Sciences, 2011).
[53]I. M. Freedberg *et al*., *Fitzpatrick's Dermatology in General Medicine*, 5th ed. (McGraw-Hill, Health Professions Division, 1999), Vol. 1.
[54]K. Sato and F. Sato, "Pharmacologic responsiveness of isolated single eccrine sweat glands," Am. J. Physiol. **240**, R44–R51 (1981).
[55]M. J. Patterson, S. D. R. Galloway, and M. A. Nimmo, "Variations in regional sweat composition in normal human males," Exp. Physiol. **85**, 869–875 (2000).
[56]J. Lieberman, "Cyclic fluctuation of sweat electrolytes in women: Effect of polythiazide upon sweat electrolytes," JAMA **195**, 629–635 (1966).
[57]J. I. Medbø and O. M. Sejersted, "Plasma potassium changes with high intensity exercise," J. Physiol. **421**, 105–122 (1990).
[58]S. R. Newmark and R. G. Dluhy, "Hyperkalemia and hypokalemia," JAMA **231**, 631–633 (1975).
[59]I. L. Schwartz and J. H. Thaysen, "Excretion of sodium and potassium in human sweat," J. Clin. Invest. **35**, 114–120 (1956).
[60]D. H. Hellhammer, S. Wüst, and B. M. Kudielka, "Salivary cortisol as a biomarker in stress research," Psychoneuroendocrinology **34**, 163–171 (2009).
[61]D. Czarnowski and J. Górski, "Sweat ammonia excretion during submaximal cycling exercise," J. Appl. Physiol. **70**, 371–374 (1991).
[62]D. Czarnowski, J. Górski, J. Jóźwiuk, and A. Boroń-Kaczmarska, "Plasma ammonia is the principal source of ammonia in sweat," Eur. J. Appl. Physiol. Occup. Physiol. **65**, 135–137 (1992).
[63]M. M. Adeva, G. Souto, N. Blanco, and C. Donapetry, "Ammonium metabolism in humans," Metabolism **61**, 1495–1511 (2012).
[64]K. Mitsubayashi, M. Suzuki, E. Tamiya, and I. Karube, "Analysis of metabolites in sweat as a measure of physical condition," Anal. Chim. Acta **289**, 27–34 (1994).
[65]S. Coyle *et al*., "BIOTEX—Biosensing textiles for personalised healthcare management," IEEE Trans. Inf. Technol. Biomed. **14**, 364–370 (2010).
[66]M. Gamella *et al*., "A novel non-invasive electrochemical biosensing device for *in situ* determination of the alcohol content in blood by monitoring ethanol in sweat," Anal. Chim. Acta **806**, 1–7 (2014).
[67]M. J. Buono, "Sweat ethanol concentrations are highly correlated with co-existing blood values in humans," Exp. Physiol. **84**, 401–404 (1999).
[68]E. Nyman and A. Palmlöv, "The elimination of ethyl alcohol in sweat," Skand. Arch. Physiol. **74**, 155–159 (1936).
[69]E. Russell, G. Koren, M. Rieder, and S. H. M. Van Uum, "The detection of cortisol in human sweat: Implications for measurement of cortisol in hair," Ther. Drug Monit. **36**, 30–34 (2014).
[70]C. Kirschbaum and D. H. Hellhammer, "Salivary cortisol," Encycl. Stress **3**, 379–383 (2000).
[71]C. Kirschbaum and D. H. Hellhammer, "Salivary cortisol in psychobiological research: An overview," Neuropsychobiology **22**, 150–169 (1989).
[72]J.-S. Raul, V. Cirimele, B. Ludes, and P. Kintz, "Detection of physiological concentrations of cortisol and cortisone in human hair," Clin. Biochem. **37**, 1105–1111 (2004).
[73]R. Keller and J. Sands, "Localization of urea transporters UT-A1 and UT-B in human eccrine clear cell (LB719)," FASEB J. **28**, LB719 (2014).
[74]Y. Y. Al-Tamer, E. A. Hadi, and I. e. I. Al-Badrani, "Sweat urea, uric acid and creatinine concentrations in uraemic patients," Urol. Res. **25**, 337–340 (1997).
[75]M. G. Bulmer, "The concentration of urea in thermal sweat," J. Physiol. **137**, 261–266 (1957).
[76]G. K. Komives, S. Robinson, and J. T. Roberts, "Urea transfer across the sweat glands," J. Appl. Physiol. **21**, 1681–1684 (1966).
[77]C.-T. Huang, M.-L. Chen, L.-L. Huang, and I. F. Mao, "Uric acid and urea in human sweat," Chin. J. Physiol. **45**, 109–115 (2002).
[78]D. A. Sakharov *et al*., "Relationship between lactate concentrations in active muscle sweat and whole blood," Bull. Exp. Biol. Med. **150**, 83–85 (2010).
[79]M. P. Ratnaparkhi, S. P. Chaudhari, and V. A. Pandya, "Peptides and proteins in pharmaceuticals," Int. J. Curr. Pharm. Res. **3**, 1–9 (2011).
[80]A. Marques-Deak *et al*., "Measurement of cytokines in sweat patches and plasma in healthy women: Validation in a controlled study," J. Immunol. Methods **315**, 99–109 (2006).
[81]E. Lee and R. D. Granstein, in *Clinical and Basic Immunodermatology*, edited by A. A. Gaspari and S. K. Tyring (Springer, London, 2008), Chap. 3, pp. 31–44.
[82]K. Tatemoto, "Neuropeptide Y and related peptides," in *Handbook of Experimental Pharmacology*, edited by M. C. Michel (Springer-Verlag, Berlin, Heidelberg, 2004), Vol. 162, Chap. 1, pp. 1–21.

[83]G. Cizza *et al*., "Elevated neuroimmune biomarkers in sweat patches and plasma of premenopausal women with major depressive disorder in remission: The POWER study," Biol. Psychiatry **64**, 907–911 (2008).
[84]H. J. Hurley and J. Witkowski, "Dye clearance and eccrine sweat secretion in human skin," J. Invest. Dermatol. **36**, 259–272 (1961).
[85]J. S. Daniels and N. Pourmand, "Label-free impedance biosensors: Opportunities and challenges," Electroanalysis **19**, 1239–1257 (2007).
[86]A. E. Kovalev, K. Dening, J. B. N. Persson, and S. N. Gorb, "Surface topography and contact mechanics of dry and wet human skin," Beilstein J. Nanotechnol. **5**, 1341–1348 (2014).
[87]A. D. Dussaud, P. M. Adler, and A. Lips, "Liquid transport in the networked microchannels of the skin surface," Langmuir **19**, 7341–7345 (2003).
[88]M. G. Bulmer and G. D. Forwell, "The concentration of sodium in thermal sweat," J. Physiol. **132**, 115–122 (1956).
[89]G. Morrison in *Clinical Methods: The History, Physical, and Laboratory Examinations*, edited by H. K. Walker, W. D. Hall, and J. W. Hurst (Butterworths, 1990), Chap. 197.
[90]K. Sato "Sweat induction from an isolated eccrine sweat gland," Am. J. Physiol. **225**, 1147–1152 (1973).
[91]J. M. Green, R. C. Pritchett, T. R. Crews, J. R. McLester, Jr., and D. C. Tucker, "Sweat lactate response between males with high and low aerobic fitness," Eur. J. Appl. Physiol. **91**, 1–6 (2004).
[92]See supplementary material at http://dx.doi.org/10.1063/1.4921039 for the derivation of the solute transport equation and sampling rate limitations for biosensors.